

Article

Not peer-reviewed version

N-Doped Carbon Nanoparticles As Antibacterial Agents: The Role of the Chemical Composition on the Antibacterial Activity

[David Lopez-Diaz](#)*, [María Dolores Merchán](#)*, [Pilar Pérez](#), [Maria Mercedes Velázquez](#)

Posted Date: 16 May 2023

doi: 10.20944/preprints202305.1085.v1

Keywords: N-doped graphene carbon nanoparticles; antibacterial ability; Escherichia coli



Preprints.org is a free multidiscipline platform providing preprint service that is dedicated to making early versions of research outputs permanently available and citable. Preprints posted at Preprints.org appear in Web of Science, Crossref, Google Scholar, Scilit, Europe PMC.

Copyright: This is an open access article distributed under the Creative Commons Attribution License which permits unrestricted use, distribution, and reproduction in any medium, provided the original work is properly cited.

Article

N-Doped Carbon Nanoparticles as Antibacterial Agents: The Role of the Chemical Composition on the Antibacterial Activity

López-Díaz, D ^{1,*}, Merchán, M.D. ^{1,2,*}, Pérez P ³ and Velázquez M.M. ^{1,2}

¹ Departamento de Química Física, Facultad de Ciencias Químicas, Universidad de Salamanca, E37008, Salamanca, Spain

² Laboratorio of Nanoelectronica and Nanomateriales, USAL-NANOLAB, Universidad de Salamanca, E37008, Salamanca, Spain

³ Instituto de Biología Funcional y Genómica, CSIC and Universidad de Salamanca, Spain

* Correspondence: authors: dld@usal.es, mdm@usal.es

Abstract: Graphene-based nanomaterials have emerged as promising materials for a wide range of applications. Therefore, in the last years carbon nanoparticles have attracted great attention due to their low toxicity, high biocompatibility and easy preparation. Recently, N-doped carbon nanoparticles have been shown to have improved antibacterial activity over the undoped nanomaterial, but it is difficult to find correlations between the structure of the nanoparticle and its antibacterial activity. With this purpose, here, we analyze the effect of both, the nanoparticle size and the surface chemical composition of four N-doped carbon nanoparticles on the growth of *Escherichia coli* bacteria. Our results were analyzed using a Ligand-Substrate model based on the Monod's equation, which allows us to interpret the dependence of the nanoparticle-bacteria affinity with the nanomaterial structure.

Keywords: N-doped graphene carbon nanoparticles; antibacterial ability; *Escherichia coli*

1. Introduction

Due to the rapid and continuous increase of the world population, increasing air and water pollution are causing infectious diseases and pathogens growing [1-4]. Likewise, the growth and adhesion of bacteria is a problem that causes a high cost in public health systems and in various industries such as clothing, biomedicine, food packaging, water treatment and filtration [5, 6]. The abuse of antibiotics such as fluoroquinolones, chloramphenicol, trimethoprim, and various carbapenem and β -lactam antibiotics, has made that many bacteria become drug resistant [7-10]. It has been proved that the mechanism of resistance in Gram-negative bacteria, such as *Escherichia coli* (*E. coli*), is based on restricting the entry of antibiotics into the cell through the outer membrane [1, 11]. Therefore, the design of new biocompatible materials as substitute of antibiotics is still a challenge.

Some metals such as Ag, Au and Pt [10, 12, 13], as well as metal oxide nanoparticles of CuO, Fe₂O₃ and ZnO [14-17] present high antibacterial activity and have been successfully used as a coating in the prevention of biofouling [18] however, their high toxicity due to the release of metal ions [13, 19, 20] discourages its use as antibacterial agents.

An alternative to metallic materials raised in the last years are the carbonaceous nanomaterials. This is because they proved to be potential bactericidal agents with low toxicity and for this reason are widely studied for their use in medicine, as carriers for drug, gene delivery or tissue engineering [9, 21-26].

In the last 10 years, many works and review articles have emerged dedicated to explore the therapeutic applications of Carbon Nanoparticles (CNPs) including graphene (G), graphene oxide (GO), reduced graphene oxide (rGO) sheets with different lateral size and thickness [24, 26-28]. Graphene (G) is a single monolayer of graphite, an atomically thick layer of sp² carbon atoms in a

honeycomb structure. Graphene can be manufactured by different methods and techniques including mechanical exfoliation, epitaxial growth, chemical vapor deposition or electrochemical methods [29-31]. However, the main drawbacks in the use of G are the cost of the processes and its water insolubility. An alternative is the oxidation of graphite with oxidizing agents such as KMnO_4 and H_2SO_4 [32-37] resulting oxygen functional groups anchored on the basal plane and on the edges of sheets. The result is a family of oxidized CNPs among which are Graphene Oxide (GO) and reduced graphene oxide (rGO). The functionalization, the size of the particles and the oxidation degree are highly dependent on the experimental conditions of the synthesis and on the starting materials used as precursors [33-37]. The oxidized carbon nanoparticles are usually soluble in polar solvents as water, dimethylformamide and dimethyl sulfoxide [38] and they have been used as basic components of nanocomposites with metals and metal oxides seeking antibacterial synergy between both materials [6].

CNPs, present different physicochemical properties due to the distinct oxidation degree and particle size that are well suited to limit microbial infection [1, 2, 6, 9, 23, 24, 26, 39, 40]. However, the antibacterial mechanisms of CNPs are still under debate. This is probably due to the great variability of its chemical composition and its morphology. When CNPs materials are in contact with bacterial cells, they can be destroyed by different mechanisms. The more accepted are the sharp edge cutting (*nanoknife*), oxidative stress, and cell trapping (wrapping). Thus, when the CNPs act through a trapping mechanism, the bacterial cells are wrapped, remaining isolated from the external environment. The isolation, restrains the access to nutrients killing the cells. This mechanism was reported for large nanoparticle size ($>10\ \mu\text{m}$) because they possess high adsorption capacity due to their higher surface energy and flexibility. Accordingly, large GO sheets demonstrated greater antimicrobial activity towards *E. coli* than the smaller ones [41]. Besides, the cell trapping mechanism is also influenced by the amphiphathic properties of the CNPs, since nanomaterial-bacteria adhesion plays an important role on the ability to wrap the bacteria [41].

The antibacterial mechanisms of CNPs can act individually or simultaneously. Besides, we think that the mechanism must be related to the material structure. It is important to consider that the size of the thinner and bigger CNPs have a complex effect on the antibacterial capacity, since they affect not only the wrapping ability but also the ability to destroy the cells through sharp edge cutting effects. These mechanisms were observed when CNPs interact with the cell wall of different bacteria, such as *E. coli* and *S. aureus*, carcinoma cells, and normal mammalian cells [9, 21, 24, 26, 41-43].

One of the most important mechanism responsible of the bacterial death is the oxidative stress [24, 44]. The mechanism is related with a charge-transfer process between CNPs and the different functional groups of the cell wall [41]. This charge-transfer process arises to imbalance between antioxidant and oxidation processes which finally kills the bacteria [45]. The mechanism depends on the presence of electronegative functional groups to induce charge transfer which can increase the generation of reactive oxygen species (ROS) [39], but also depends on the other structural properties such as size, the oxidation degree [1], or the surface curvature of nanoparticles [46].

We are interested to study the role of the chemical composition on the antibacterial activity. Therefore, we analyze the antibacterial activity of four carbon nanoparticles containing different Nitrogen (N-) and Oxygen(O-) functional groups against *Escherichia Coli*. We have selected N-doped carbon nanoparticles synthesized from four different carbon precursors using the acid oxidative synthesis, since we have proved in a previous work that both size and chemical composition depends on the precursorprecursors [47].

We have preferred N-Doped nanoparticles over undoped ones, because some N-groups are electron donor that could favor the charge-transfer processes. Besides, we have designed a new synthesis methodology based on the acid oxidative process of different carbon precursors which allow obtaining material with different chemical composition and size [47]. Therefore, we expect that the analysis of the antibacterial activity of these CNPs allows us the deep understanding of the physicochemical bases underlying the bacteria-nanoparticle interactions, facilitate the design of antibacterial agents based on carbon compounds, clarifying the relationship between the structure and the antibacterial mechanism of these materials.

2. Materials and Methods

2.1. Materials and reagents

To modulate the size and chemical composition of carbon nanoparticles, CNPs, four starting materials were selected: three commercial graphite samples and one helical carbon nanofibers. The graphite samples were natural graphite flakes, 99.02 C fixed, supplied by Qingdao super graphite Co. LTD; and graphite powder of < 20-micron particle size and highly oriented pyrolytic graphite (HOPG) supplied by Sigma Aldrich (St. Louis, MO). Non-graphitized GANF® helical ribbon carbon nanofibers have been gifted by Carbon Advanced Materials, Grupo Antolín (Spain). GANF® are synthesized by CVD using the floating catalyst method [48].

Reagents HNO₃ (65%), H₂SO₄ (98%), Na₂CO₃ and HCl (35%) were provided by Sigma Aldrich and used without further purification.

To select a given size of the nanoparticles, a Spectra/Por® 6 Standard RC 2 kDa dialysis bag supplied by Spectrum Labs (California, USA) was used. To prepare solutions and reagents for oxidation, ultrapure water prepared with a combination of Millipore's RiOs and Milli-Q systems was used. The conductivity of the water was less than 0.2 µS/cm and its surface tension value was 72.5 mNm⁻¹.

2.2. Synthesis of CNPs

CNPs were synthesized using the acidic oxidative process previously reported [47, 49]. Briefly, 0.30 g of the graphitic materials were dispersed into a mixture of H₂SO₄ (60 ml) and HNO₃ (20 ml). To obtain a homogeneous solution, the mixtures were sonicated for two hours and further stirred for 24 hours at 100°C. Then, the brown solution becomes transparent since the graphitic material is completely dissolved.

The transparent solution was cooled at room temperature and diluted with MilliQ ultra-pure water (800 ml). The pH was adjusted to 8 by adding Na₂CO₃ and the color of the solutions changed from brown to light yellow. Finally, the solutions were filtered and further dialyzed for 3 days in a dialysis bag (retained molecular weight: 2 k Da). The list of acronyms corresponding to each material can be found in abbreviation list. The concentrations of aqueous solutions after dialysis were 0.45 (CNPNF) mg/ml, 0.28 (CNPPW) mg/ml, 0.21 (CNPHPG) mg/ml and 0.44 (CNPG) mg/ml.

2.3. X-ray photoelectronic spectroscopy (XPS) measurements

The XPS spectra of solid materials were recorded in a VG Escalab 200R spectrophotometer (Fison Instrument, Parkton, MD, USA). The source excitation was a MgKα (hν=1253.6 eV). The equipment uses a hemispherical electron analyzer. The residual pressure inside the analysis chamber during the acquisition was kept under 4x 10⁻⁷ Pa. To record the high-resolution spectra, the analyzer pass energy was 20 KeV.

2.4. Antibacterial test

The antibacterial activity of the CNPs was evaluated against the Gram-negative bacteria *Escherichia coli* (*E. Coli* DH5α) following the methodology in reference [50] including slightly modifications. Briefly, *E. Coli* grown in Luria-Bertoni (LB) media was incubated at (10⁻⁶ bacteria / ml) with fresh solutions of CNPs during 1 h at 37°C. The CNP concentrations in the LB medium varied between 10 and 60 µg/ml. Subsequently, the bacteria were diluted 100 times and aliquots containing about 125 bacteria were withdrawn and spread in 25 ml LB-agar plates. These plates were incubated at 37 °C during 24 h and then, the antibacterial activity was evaluated by colony counting method. The colonies were counted and compared with those on control plated without carbon nanoparticles, then, the antibacterial capacity was calculated in terms of reduction rate percentage from the following equation [5]

$$\text{Reduction rate \%} = \frac{N_{\text{control}} - N_{\text{sample}}}{N_{\text{control}}} \times 100 \quad (1)$$

In Eq. 1 N_{control} and N_{sample} represent the number of colonies from the control, without CNP, and for each CNP sample respectively as a function of the concentration. All treatments were prepared in duplicate and repeated at least three times for each sample and were done in dark. Data in graphic represent the averaged values and the error bars are the standard deviations.

3. Results

N-CNPs were characterized by X-ray photoelectron spectroscopy (XPS) to determine their surface composition and transmission electron microscopy (SEM) and Tracking analysis (NTA) to obtain the nanoparticles size. The results are collected in Table 1 and show the strong influence of the starting material used in the synthesis on the morphology of the CNPs that we obtain.

Table 1. Structural properties of CNPs.

Materials	Precursor	Diameter ¹ / nm	Amine groups ¹ % (XPS)	Imine groups ¹ % (XPS)	K/mg ⁻¹ l	Chi-Sqr
CNPNF	Carbon nanofibers	9.3 ± 0.9	47 ± 3	32 ± 3	0.043±0.007	0.942
CNPPW	Graphite powder	93.6 ± 3.8	36 ± 3	22 ± 2	0.030±0.005	0.955
CNPHPG	Pyrolytic graphite	52.0 ± 1	21 ± 2	16 ± 1	0.29±0.005	0.967
CNPG	Graphite flakes	85.3 ± 1.1	35 ± 3	30 ± 3	0.032±0.005	0.981

¹ Data from ref. [39].

To study the effect of the concentration on the bactericide activity of CNPs, *E. coli* bacteria were incubated at 37 °C with different CNPs concentrations in the range of 10 to 60 µg/ml during 1h, and were spread in plates with LB-agar, for more details see Experimental Section. Figure 1 shows the evolution of the number of colonies with the nanomaterial concentration. The number of colonies were obtained by the counting method. As control, a plate without CNPs was prepared following the described protocol. At insets of the figure, a representative image of the plates with colonies are also included.

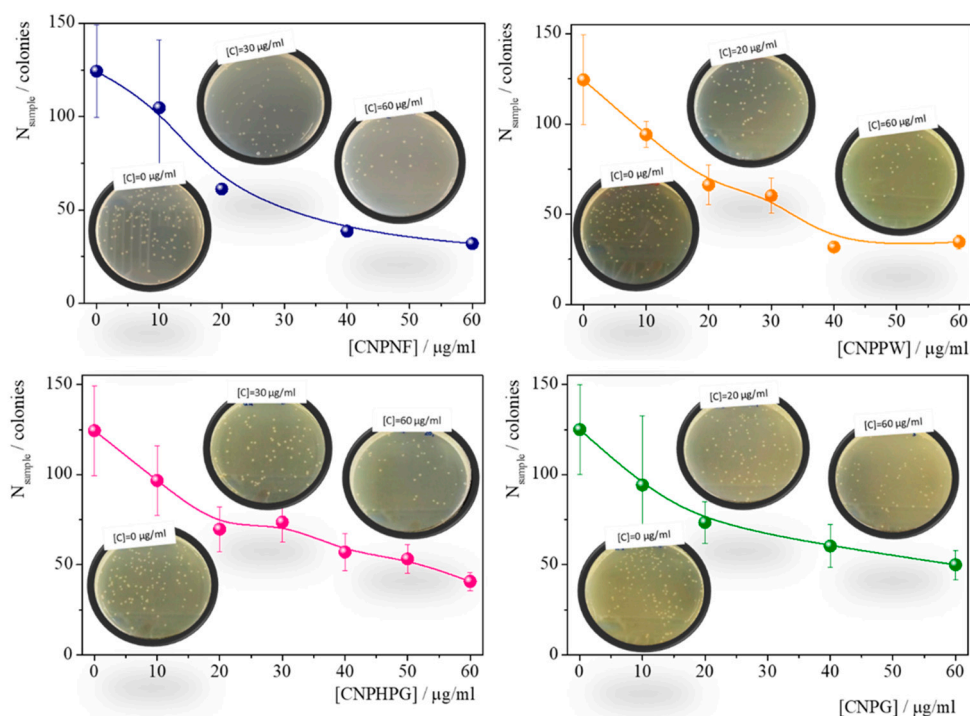


Figure 1. Evolution of the number of bacterial colonies with the CNPs concentration. The pictures of plates containing bacteria colonies are as inset in the figures.

As shown in Figure 1, the number of colonies decreases with the nanoparticle concentration and the variation with concentration seems to be different for each material. To quantify the differences between samples, we calculate the reduction rate percentage value using the Equation 1, [51] and the values are plotted against the nanoparticle concentration in Figure 2.

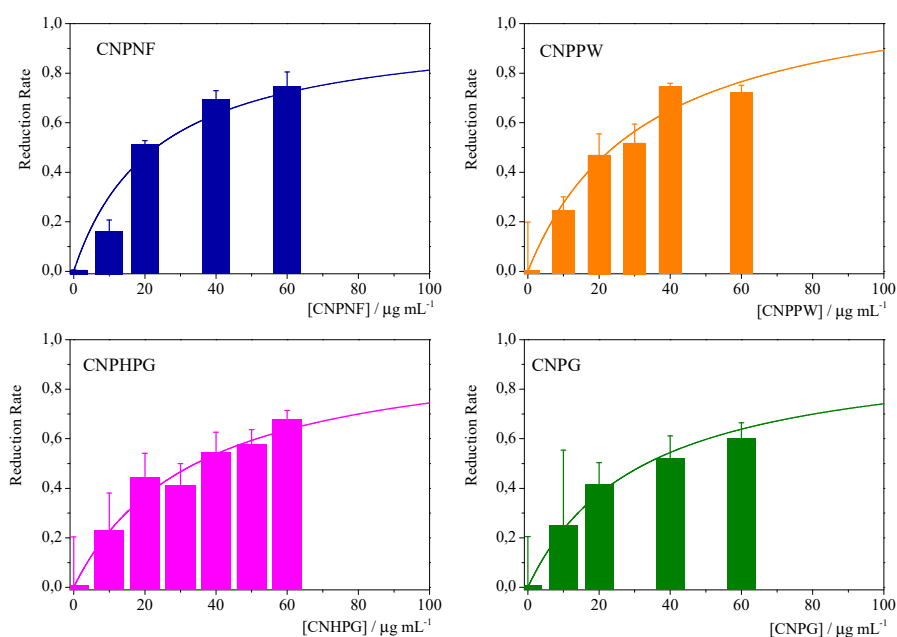
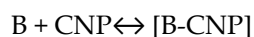


Figure 2. Variation of the antibacterial capacity in terms of the reduction percentage values, eq. 1, with the carbon nanoparticle concentration. Lines represent the best fit of the reduction rate against the concentration of CNP according to the Monod's model.

4. Discussion

As can be seen in Figure 2, the reduction rate of antibacterial capacity increases with nanoparticle concentration until saturation at a given CNP concentration. However, the concentration dependence seems to be different for each material. We want to interpret this behavior from a physicochemical point of view and to clarify the mechanisms acting between CNPs and bacteria. Therefore, we assume that the bacteria death could be due to interactions between the chemical groups of the bacterial wall and the functional groups of the nanomaterials. Accordingly, the rate of formation of the complex [Bacteria-nanoparticle] could be proportional to the reduction rate because if the complex B-CNP is formed, the bacteria dead. We also assume a reversible equilibrium between bacteria (B) and nanoparticles (CNP) and the complex, [B-CNP].



This equilibrium is studied using a mathematical model based on the Monod's equation in terms of the reduction rate of the colony, RR [52, 53].

$$RR = \frac{RR_{max} [CNP]}{1/K + [CNP]} \quad (2)$$

In equation 2, RR_{max} represents the maximum reduction rate and K is the complex formation equilibrium constant which provides a measure of the affinity between nanoparticles and bacteria hereinafter, affinity constant.

The results of the reduction rate (Figure 2) have been fitted to the Monod's model (Equation 2). The simulated curves have been also inserted in figure 2 and parameters obtained in fits (K and Chi-sqr) are collected in Table 1. As can be seen in Figure 3, the model fits acceptably our experimental results.

Data show that the shape of the reduction rate (Figure 2), as well as the values of the affinity constant obtained from the fits depend on the nanomaterial used as antibacterial agent. This means that the bactericidal activity could be related to the chemical composition and/or the nanomaterial size. To check these issues, we have plotted at Figure 3 the affinity constant, K, against the the sum of the percentage of amine and imine groups and againsts the diameter of nanoparticles (data taken from Table 1). Results in Figure 3a indicate a correlation between the affinity constant and the sum of the percentage of amine and imine groups. This behavior is consistent with results previously reported in which it is assumed that N groups of the nanoparticle interact with the cell [54] by electron-transfer processes. Accordingly, when the amine and imine groups in the material increase, the number of N atoms with non-bonding electrons also increases favoring the interactions between the material and bacteria by electron charge mechanism. These electron transfer processes induce a disturbance of the bacterial enzymes, the so-called oxidative stress mechanism [54].

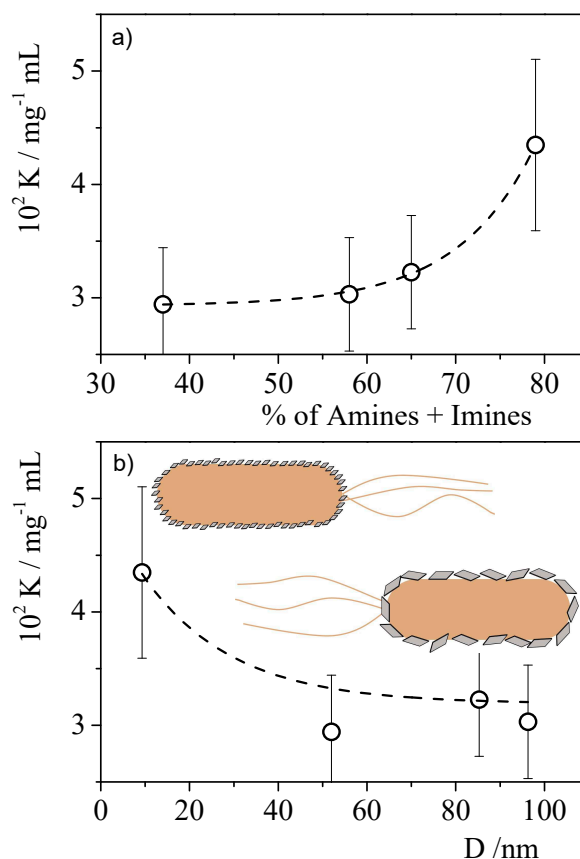


Figure 3. Evolution of the affinity constant, K with a) the percentage of Amines and Imines, b) the size of the N-doped nanoparticles.

It is interesting to note, that the bactericidal character of nanoparticles comes from the chemical interaction between the N- functional groups attached to the wall of the bacteria, it would be expected that the nanoparticle size would also play an important role in the reduction rate. In Figure 3b we can observe that the affinity constant decreases as the diameter of nanoparticle increases. This point to the existence of an additional mechanism. According to the results in Figure 3b, a wrapping mechanism could be ruled out, since in that case, the bactericidal power, and consequently, the affinity constant, should increase with size. Since the affinity constant decreases when the size of the nanoparticles increases, the behavior could be interpreted by the nanoknife mechanism acting simultaneously with the oxidative stress. Other interpretation could be to assume a steric hindrance which hinders the encounter between the reactive groups located at the bacteria wall and the N-groups of the nanomaterials; however, using our results it is not possible to conclude about the origin of this second mechanism [24].

5. Conclusions

We have designed N-doped carbon nanoparticles as antibacterial agents using the acid oxidative synthesis previously reported and four carbon precursors, resulting nanomaterials with different chemical composition, N- and O-groups, and distinct diameters. Using these four different materials, we have analyzed the influence of the material structure on the antibacterial activity against *Escherichia coli* bacteria. Our results prove that the antibacterial activity increases as the nanoparticle concentration increases. The behavior was modeled by the Monod's equation considering the formation of a complex between the chemical groups of bacteria and nanoparticles. From the dependence of the affinity constant calculated obtained from the model with the percentage of amine and imine groups of the nanomaterials was possible to conclude that the mechanism of the

antibacterial activity can be related to oxidative stress produced by the electron-transfer processes between N-groups of the nanomaterial and the functional groups of the bacteria. Our results also show the existence of an additional mechanism, probably nanoknife or steric hindrance, acting simultaneously with the oxidative stress. Using our results, it was not possible to discern the nature of this second mechanism. More experimental efforts are necessary to elucidate its origin. However, the chemical synthesis for obtaining nanomaterials with a given chemical structure and size is not easy. Physical methods of CNPs preparation such as lithography or ultrasounds treatment could provide a good way to modulate the structure of these nanomaterials. This strategy will be used in future works to confirm the existence of these mechanisms.

Author Contributions: Conceptualization, DLD, and MMV.; methodology, PP, DLD, and MMV; investigation, PP, DLD, MDM, and MMV; data curation, DLD, MDM, and MMV; writing—original draft preparation, DLD, MDM, and MMV; writing—review and editing, DLD, MDM, PP, and MMV; funding acquisition, MMV. All authors have read and agreed to the published version of the manuscript.

Funding: This research was funded by European Regional Development Fund, ERDF, and Junta de Castilla y León grant number SA121P20 and MINECO, grants CTQ2016-78895-R and PGC2018-098924-B-100.

Acknowledgments: Authors thank Dr. García Fierro (Instituto de Catálisis y Petroleoquímica, Madrid) for XPS measurements.

Conflicts of Interest: The authors declare no conflict of interest.

Abbreviations: CNPNF carbon nanoparticles synthesized from GANF carbon nanofibers (non-graphitized), CNPPW carbon nanoparticles synthesized from graphite powers, CNPHPG carbon nanoparticles synthesized from Highly Oriented Pyrolytic Graphite, CNPG carbon nanoparticles synthesized from graphite flakes, G: Graphene.

GO: Graphene Oxide.

rGO: Reduced Graphene Oxide

N-CNP: N-doped carbon nanoparticles

CNP: Carbon Nanoparticle

ROS: Reactive Oxidative Species

XPS: X-ray photoelectronic spectroscopy

TEM: Transmission electron microscopy

NTA: Nanoparticle tracking analysis

References

1. Anand, A.; Unnikrishnan, B.; Wei, S.-C.; Chou, C. P.; Zhang, L.-Z.; Huang, C.-C., Graphene oxide and carbon dots as broad-spectrum antimicrobial agents – a minireview. *Nanoscale Horiz.* **2019**, *4*, (1), 117-137.
2. Fatima, N.; Qazi, U. Y.; Mansha, A.; Bhatti, I. A.; Javaid, R.; Abbas, Q.; Nadeem, N.; Rehan, Z. A.; Noreen, S.; Zahid, M., Recent developments for antimicrobial applications of graphene-based polymeric composites: A review. *Journal of Industrial and Engineering Chemistry* **2021**, *100*, 40-58.
3. Dong, A.; Wang, Y.-J.; Gao, Y.; Gao, T.; Gao, G., Chemical Insights into Antibacterial N-Halamines. *Chem. Rev.* **2017**, *117*, (6), 4806-4862.
4. Zhang, X.; Kong, H.; Yang, G.; Zhu, D.; Luan, X.; He, P.; Wei, G., Graphene-Based Functional Hybrid Membranes for Antimicrobial Applications: A Review. *Applied Sciences* **2022**, *12*, (10).
5. Díez-Pascual, A. M., Antibacterial Activity of Nanomaterials. *Nanomaterials (Basel, Switzerland)* **2018**, *8*, (6), 359.
6. Díez-Pascual, A. M., Antibacterial Action of Nanoparticle Loaded Nanocomposites Based on Graphene and Its Derivatives: A Mini-Review. *International Journal of Molecular Sciences* **2020**, *21*, (10).
7. Fair, R. J.; Tor, Y., Antibiotics and Bacterial Resistance in the 21st Century. *Perspect Medicin Chem* **2014**, *6*, PMC.S14459.

8. Kavanagh, K. T.; Calderon, L. E.; Saman, D. M.; Abusalem, S. K., The use of surveillance and preventative measures for methicillin-resistant staphylococcus aureus infections in surgical patients. *Antimicrobial Resistance and Infection Control* **2014**, *3*, (1), 18.
9. Ji, H.; Sun, H.; Qu, X., Antibacterial applications of graphene-based nanomaterials: Recent achievements and challenges. *Advanced Drug Delivery Reviews* **2016**, *105*, 176-189.
10. Zheng, K.; Setyawati, M. I.; Leong, D. T.; Xie, J., Antimicrobial Gold Nanoclusters. *ACS Nano* **2017**, *11*, (7), 6904-6910.
11. Miller, S. I., Antibiotic Resistance and Regulation of the Gram-Negative Bacterial Outer Membrane Barrier by Host Innate Immune Molecules. *mBio* **2016**, *7*, (5), e01541-16.
12. Hoseinnejad, M.; Jafari, S. M.; Katouzian, I., Inorganic and metal nanoparticles and their antimicrobial activity in food packaging applications. *null* **2018**, *44*, (2), 161-181.
13. Zheng, K.; Setyawati, M. I.; Leong, D. T.; Xie, J., Surface Ligand Chemistry of Gold Nanoclusters Determines Their Antimicrobial Ability. *Chem. Mater.* **2018**, *30*, (8), 2800-2808.
14. Raghunath, A.; Perumal, E., Metal oxide nanoparticles as antimicrobial agents: a promise for the future. *International Journal of Antimicrobial Agents* **2017**, *49*, (2), 137-152.
15. Sirelkhatim, A.; Mahmud, S.; Seeni, A.; Kaus, N. H. M.; Ann, L. C.; Bakhori, S. K. M.; Hasan, H.; Mohamad, D., Review on Zinc Oxide Nanoparticles: Antibacterial Activity and Toxicity Mechanism. *Nano-Micro Letters* **2015**, *7*, (3), 219-242.
16. Liu, J.; Wang, Y.; Ma, J.; Peng, Y.; Wang, A., A review on bidirectional analogies between the photocatalysis and antibacterial properties of ZnO. *Journal of Alloys and Compounds* **2019**, *783*, 898-918.
17. Chankhanittha, T.; Nanan, S., Visible-light-driven photocatalytic degradation of ofloxacin (OFL) antibiotic and Rhodamine B (RhB) dye by solvothermally grown ZnO/Bi₂MoO₆ heterojunction. *Journal of Colloid and Interface Science* **2021**, *582*, 412-427.
18. Liu, Z.; Zheng, X.; Zhang, H.; Li, W.; Jiang, R.; Zhou, X., Review on formation of biofouling in the marine environment and functionalization of new marine antifouling coatings. *Journal of Materials Science* **2022**, *57*, (39), 18221-18242.
19. Wang, D.; Lin, Z.; Wang, T.; Yao, Z.; Qin, M.; Zheng, S.; Lu, W., Where does the toxicity of metal oxide nanoparticles come from: The nanoparticles, the ions, or a combination of both? *Journal of Hazardous Materials* **2016**, *308*, 328-334.
20. Soenen, S. J.; Parak, W. J.; Rejman, J.; Manshian, B., (Intra)Cellular Stability of Inorganic Nanoparticles: Effects on Cytotoxicity, Particle Functionality, and Biomedical Applications. *Chem. Rev.* **2015**, *115*, (5), 2109-2135.
21. Tu, Y.; Lv, M.; Xiu, P.; Huynh, T.; Zhang, M.; Castelli, M.; Liu, Z.; Huang, Q.; Fan, C.; Fang, H.; Zhou, R., Destructive extraction of phospholipids from Escherichia coli membranes by graphene nanosheets. *Nature Nanotechnology* **2013**, *8*, (8), 594-601.
22. Bitounis, D.; Ali-Boucetta, H.; Hong, B. H.; Min, D.-H.; Kostarelos, K., Prospects and Challenges of Graphene in Biomedical Applications. *Advanced Materials* **2013**, *25*, (16), 2258-2268.
23. Shi, L.; Chen, J.; Teng, L.; Wang, L.; Zhu, G.; Liu, S.; Luo, Z.; Shi, X.; Wang, Y.; Ren, L., The Antibacterial Applications of Graphene and Its Derivatives. *Small* **2016**, *12*, (31), 4165-4184.
24. Zou, X.; Zhang, L.; Wang, Z.; Luo, Y., Mechanisms of the Antimicrobial Activities of Graphene Materials. *J. Am. Chem. Soc.* **2016**, *138*, (7), 2064-2077.
25. Jian, H.-J.; Wu, R.-S.; Lin, T.-Y.; Li, Y.-J.; Lin, H.-J.; Harroun, S. G.; Lai, J.-Y.; Huang, C.-C., Super-Cationic Carbon Quantum Dots Synthesized from Spermidine as an Eye Drop Formulation for Topical Treatment of Bacterial Keratitis. *ACS Nano* **2017**, *11*, (7), 6703-6716.
26. Xin, Q.; Shah, H.; Nawaz, A.; Xie, W.; Akram, M. Z.; Batool, A.; Tian, L.; Jan, S. U.; Boddula, R.; Guo, B.; Liu, Q.; Gong, J. R., Antibacterial Carbon-Based Nanomaterials. *Advanced Materials* **2019**, *31*, (45), 1804838.
27. Hu, W.; Peng, C.; Luo, W.; Lv, M.; Li, X.; Li, D.; Huang, Q.; Fan, C., Graphene-Based Antibacterial Paper. *ACS Nano* **2010**, *4*, (7), 4317-4323.
28. Krishnamoorthy, K.; Veerapandian, M.; Yun, K.; Kim, S. J., The chemical and structural analysis of graphene oxide with different degrees of oxidation. *Carbon* **2013**, *53*, 38-49.
29. Weiss, N. O.; Zhou, H.; Liao, L.; Liu, Y.; Jiang, S.; Huang, Y.; Duan, X., Graphene: An Emerging Electronic Material (Adv. Mater. 43/2012). *Advanced Materials* **2012**, *24*, (43), 5776-5776.
30. Kuilla, T.; Bhadra, S.; Yao, D.; Kim, N. H.; Bose, S.; Lee, J. H., Recent advances in graphene based polymer composites. *Progress in Polymer Science* **2010**, *35*, (11), 1350-1375.
31. Zheng, Q.; Kim, J.-K., Synthesis, Structure, and Properties of Graphene and Graphene Oxide. In *Graphene for Transparent Conductors: Synthesis, Properties and Applications*, Zheng, Q.; Kim, J.-K., Eds. Springer New York: New York, NY, 2015; pp 29-94.
32. Martin-Garcia, B.; Velazquez, M. M.; Rossella, F.; Bellani, V.; Diez, E.; Garcia Fierro, J. L.; Perez-Hernandez, J. A.; Hernandez-Toro, J.; Claramunt, S.; Cirera, A., Functionalization of reduced graphite oxide sheets with a zwitterionic surfactant. *Chemphyschem* **2012**, *13*, (16), 3682-90.

33. Lopez-Diaz, D.; Velazquez, M. M.; Blanco de La Torre, S.; Perez-Pisonero, A.; Trujillano, R.; Garcia Fierro, J. L.; Claramunt, S.; Cirera, A., The role of oxidative debris on graphene oxide films. *Chemphyschem* **2013**, *14*, (17), 4002-9.
34. Hidalgo, R. S.; López-Díaz, D.; Velázquez, M. M., Graphene Oxide Thin Films: Influence of Chemical Structure and Deposition Methodology. *Langmuir* **2015**, *31*, (9), 2697-2705.
35. Claramunt, S.; Varea, A.; López-Díaz, D.; Velázquez, M. M.; Cornet, A.; Cirera, A., The Importance of Interbands on the Interpretation of the Raman Spectrum of Graphene Oxide. *J. Phys. Chem. C* **2015**, *119*, (18), 10123-10129.
36. López-Díaz, D.; López Holgado, M.; García-Fierro, J. L.; Velázquez, M. M., Evolution of the Raman Spectrum with the Chemical Composition of Graphene Oxide. *J. Phys. Chem. C* **2017**, *121*, (37), 20489-20497.
37. López-Díaz, D.; Merchán, M. D.; Velázquez, M. M., The behavior of graphene oxide trapped at the air water interface. *Advances in Colloid and Interface Science* **2020**, *286*, 102312.
38. Dreyer, D. R.; Park, S.; Bielawski, C. W.; Ruoff, R. S., The chemistry of graphene oxide. *Chem Soc Rev* **2010**, *39*, (1), 228-40.
39. Kuo, W.-S.; Shao, Y.-T.; Huang, K.-S.; Chou, T.-M.; Yang, C.-H., Antimicrobial Amino-Functionalized Nitrogen-Doped Graphene Quantum Dots for Eliminating Multidrug-Resistant Species in Dual-Modality Photodynamic Therapy and Bioimaging under Two-Photon Excitation. *ACS Applied Materials & Interfaces* **2018**, *10*, (17), 14438-14446.
40. Yaragalla, S.; Bhavitha, K. B.; Athanassiou, A., A Review on Graphene Based Materials and Their Antimicrobial Properties. *Coatings* **2021**, *11*, (10).
41. Liu, S.; Zeng, T. H.; Hofmann, M.; Burcombe, E.; Wei, J.; Jiang, R.; Kong, J.; Chen, Y., Antibacterial Activity of Graphite, Graphite Oxide, Graphene Oxide, and Reduced Graphene Oxide: Membrane and Oxidative Stress. *ACS Nano* **2011**, *5*, (9), 6971-6980.
42. Akhavan, O.; Ghaderi, E.; Esfandiar, A., Wrapping Bacteria by Graphene Nanosheets for Isolation from Environment, Reactivation by Sonication, and Inactivation by Near-Infrared Irradiation. *J. Phys. Chem. B* **2011**, *115*, (19), 6279-6288.
43. Akhavan, O.; Ghaderi, E.; Akhavan, A., Size-dependent genotoxicity of graphene nanoplatelets in human stem cells. *Biomaterials* **2012**, *33*, (32), 8017-8025.
44. Rojas-Andrade, M. D.; Chata, G.; Rouholiman, D.; Liu, J.; Saltikov, C.; Chen, S., Antibacterial mechanisms of graphene-based composite nanomaterials. *Nanoscale* **2017**, *9*, (3), 994-1006.
45. Li, Y.-J.; Harroun, S. G.; Su, Y.-C.; Huang, C.-F.; Unnikrishnan, B.; Lin, H.-J.; Lin, C.-H.; Huang, C.-C., Synthesis of Self-Assembled Spermidine-Carbon Quantum Dots Effective against Multidrug-Resistant Bacteria. *Advanced Healthcare Materials* **2016**, *5*, (19), 2545-2554.
46. Hui, L.; Huang, J.; Chen, G.; Zhu, Y.; Yang, L., Antibacterial Property of Graphene Quantum Dots (Both Source Material and Bacterial Shape Matter). *ACS Applied Materials & Interfaces* **2016**, *8*, (1), 20-25.
47. López-Díaz, D.; Solana, A.; García-Fierro, J. L.; Merchán, M. D.; Velázquez, M. M., The role of the chemical composition on the photoluminescence properties of N-doped carbon nanoparticles. *Journal of Luminescence* **2020**, *219*, 116954.
48. Vera-Agullo, J.; Varela-Rizo, H.; Conesa, J. A.; Almansa, C.; Merino, C.; Martin-Gullon, I., Evidence for growth mechanism and helix-spiral cone structure of stacked-cup carbon nanofibers. *Carbon* **2007**, *45*, (14), 2751-2758.
49. Peng, J.; Gao, W.; Gupta, B. K.; Liu, Z.; Romero-Aburto, R.; Ge, L.; Song, L.; Alemany, L. B.; Zhan, X.; Gao, G.; Vithayathil, S. A.; Kaipparettu, B. A.; Marti, A. A.; Hayashi, T.; Zhu, J.-J.; Ajayan, P. M., Graphene Quantum Dots Derived from Carbon Fibers. *Nano Letters* **2012**, *12*, (2), 844-849.
50. Akhavan, O.; Ghaderi, E., Escherichia coli bacteria reduce graphene oxide to bactericidal graphene in a self-limiting manner. *Carbon* **2012**, *50*, (5), 1853-1860.
51. Bao, Q.; Zhang, D.; Qi, P., Synthesis and characterization of silver nanoparticle and graphene oxide nanosheet composites as a bactericidal agent for water disinfection. *Journal of Colloid and Interface Science* **2011**, *360*, (2), 463-470.
52. Merchuk, J. C.; Asenjo, J. A., The Monod equation and mass transfer. *Biotechnol Bioeng* **1995**, *45*, (1), 91-4.
53. Tan, Y.; Wang, Z.-X.; Schneider, R.; Marshall, K. C., Modelling microbial growth: A statistical thermodynamic approach. *Journal of Biotechnology* **1994**, *32*, (2), 97-106.
54. Dwitya, S. S.; Hsueh, Y.-H.; Wang, S. S. S.; Lin, K.-S., Ultrafine nitrogen-doped graphene quantum dot structure and antibacterial activities against Bacillus subtilis 3610. *Materials Chemistry and Physics* **2023**, *295*, 127135.

Disclaimer/Publisher's Note: The statements, opinions and data contained in all publications are solely those of the individual author(s) and contributor(s) and not of MDPI and/or the editor(s). MDPI and/or the editor(s) disclaim responsibility for any injury to people or property resulting from any ideas, methods, instructions or products referred to in the content.